Characterization of femtosecond-laser-induced periodic structures on SiC substrates

Reina Miyagawa[1*], Yutaka Ohno[2], Momoko Deura[2], Ichiro Yonenaga[2] and Osamu Eryu[1]

[1] Department of Physical Science and Engineering, Nagoya Institute of Technology, Nagoya 466–8555, Japan

[2] Institute for Materials Research, Tohoku University, Sendai 980–8577, Japan

[*]E-mail: miyagawa.reina@nitech.ac.jp

Abstract

We investigated the crystalline state of femtosecond-laser-induced periodic structures using a transmission electron microscope (TEM). The core of the 200-nm-pitch periodic nanostructures on SiC retained a high crystalline quality continued from the SiC substrate, where the crystal orientation was aligned with that of the SiC substrate. These results suggest that the periodic nanostructures were formed by periodic etching and not by rearrangement. At high laser power, amorphous microstructures with sizes larger than 2 μm were formed on the periodic nanostructures. The microstructures were amorphous and extended from the amorphous SiC layer that covered the periodic nanostructures.

1. Introduction

Femtosecond-laser processing has been applied in a wide range of fields [1-3]. Recently, periodic nanostructures, formed using femtosecond-laser irradiation, have attracted much interest as laser-induced periodic surface structures (LIPSS) [4-16]. The periodicity of the nanostructures thus formed is less than the wavelength of the incident laser. Several LIPSS-formation mechanisms have been proposed, including the excitation of surface plasmon polaritons (SPPs) [7-12], second harmonic generation (SHG) [13-15], and a parametric-decay process [16]. The precise mechanism involved remains under debate because it is believed that the structures are formed through several interactions. Previous research on laser irradiation of Si includes investigation of a laser-induced damage layer that is dependent on the number of superimposed pulses [17-20]. In this study, we investigated the dependence of laser fluence on the crystalline states of LIPSS on SiC using a TEM. Understanding the crystalline state could be beneficial for comprehending the formation mechanism such the structures. A SiC substrate was used as an irradiated material. SiC, with a wide bandgap, is an attractive material for use in high-temperature, high-speed, and high-voltage devices. Recent progress in SiC crystal growth has shown that it is possible to prepare a single-crystal SiC substrate [21-24]. SiC is useful for investigating the direct effect of laser irradiation on a material because it is physically and chemically stable. Moreover, as a result of progress in crystal growth and surface conditioning, such as chemical-mechanical polishing (CMP), high-quality SiC substrates with a surface flattened down to the atomic level and no micropipe defects are now available. This surface flatness is the premise for investigating surface-effective functions such as SPPs. SiC is a processing-resistant material because of its high hardness and wide-bandgap. Here, we propose non-thermal and nonlinear processing using a femtosecond laser. This processing method could be applied widely, such as hard materials or

transparent materials. Furthermore, a maskless process may extend the possibility of forming desired structures.

2. Experimental procedure

Laser irradiation was performed using a femtosecond-laser oscillator (IMRA America, μ jewel D-10K; λ = 1045 nm, T_{pw} = 450 fs, f = 100–1000 kHz, where λ, T_{pw}, and f are the wavelength, pulse width, and repetition frequency of incident laser, respectively). A 6H-SiC wafer was used as the substrate. The surface-crystallographic orientation was (0001) and the material was doped with nitrogen. The substrate surface was treated by CMP. A laser beam was focused by a collective lens for irradiation onto the surface of the SiC substrate at its focal point. The beam diameter at the focal point was estimated to be approximately 15 μm. The SiC substrate was irradiated while being linearly scanned at a rate of approximately 1 cm/s in air. The numbers of superimposed pulses on the SiC substrate were approximately 150 (f = 100 kHz) and 1500 (f = 1000 kHz). Based on previous research [25], periodic structures on the SiC substrate were formed with high reproducibility by superimposed laser irradiation. Before and after irradiation, a wet-etching process using acetone for 10 min, hydrofluoric acid (50 wt%) for 20 min, ultrapure water for 10 min, and isopropyl alcohol for 10 min was performed. The TEM observation was performed using a JEOL JEM-2000EX at an accelerating voltage of 160 kV, and the high-resolution TEM observation was performed using a JEOL JEM-ARM200F at an accelerating voltage of 200 kV. The samples for TEM observation were prepared using a focused-ion-beam (FIB) processing machine (JEOL JEM-9320FIB). The morphology of the structures was observed using a scanning electron microscope (SEM; JEOL JSM-7800F).

3. Results and discussion

The cross-sectional SEM images of the 6H-SiC substrate irradiated at each average laser power and repetition frequency are shown in Fig. 1. As parameters, the average laser power and repetition frequency were varied from 0.2–4.0 W and 100–1000 kHz, respectively. Figures 1(a) and 1(b) show a high-resolution image irradiated at 0.5 W and 500 kHz and at 4.0 W and 1000 kHz, respectively. The direction of the laser polarization is shown as arrow *E* in Fig. 1. Laser-induced periodic structures were formed on the SiC substrates. The direction of the periodic nanostructures was perpendicular to the polarization direction of the incident laser. According to previous research [6], the direction of the periodic nanostructures is dependent on the laser polarization and not on the in-plane direction of the SiC substrate or the direction of laser scanning. At high laser peak intensity (i.e. at high average laser power or at low repetition frequency) calculated using Eq. (1), SiC substrates were ablated in a "v" shape.

$$\text{peak intensity} = \frac{\text{average power}}{\text{repetition frequency} \times \text{pulse duration} \times \text{spot area}} \quad (1)$$

The laser-induced periodic structures were formed on the sidewalls and bottom of the v-shaped ablation trench. Though the width of the laser-induced structures tends to increase with increasing the laser power, it was approximately 10–20 μm, which nearly same as the diameter of the laser. As shown in the enlarged SEM image in Fig. 1(b), microstructures with sizes larger than 5 μm were formed on the periodic nanostructures with irradiation at high peak intensity. We discuss the crystalline states and formation process for those structures with respect to peak intensity.

The periodicity of the nanostructures is shown in Fig. 2. The periodicity was approximately 200–300 nm. Although less dependent on the laser peak intensity, the

distribution increased with increasing average laser power. Figure 3 shows TEM images of the periodic nanostructures on the SiC substrate irradiated at an average power of 0.5 W and a repetition frequency of 500 kHz. Figure 3(a) shows the bright-field TEM image, where the black grains on the periodic nanostructures are tungsten, a by-product of the FIB. The core of the periodic nanostructures was crystalline, comparable to the SiC substrate, as shown in the high-resolution TEM image in Fig. 3(b) and the diffraction patterns of the periodic nanostructures and SiC substrate in Fig. 3(c). The periodic nanostructures were covered with an amorphous SiC layer with a thickness of 20–50 nm, similar to previous studies [26]. This amorphous SiC layer may have been formed by a reaction with the atmosphere or thermal damage. Taking into consideration the optical-penetration and skin depths for electromagnetic frequencies [27], we consider reaction with the atmosphere to be an effective explanation. The interface between the crystalline and amorphous regions was steep, where the crystalline region was not damaged by laser irradiation, as clearly shown in the atomic image in Fig. 3(b). Moreover, the crystalline region of the periodic nanostructures was a continuation from the SiC substrate, where the crystal orientation of the core of the periodic nanostructures was aligned with that of the SiC substrate and it keeps 6H-SiC crystalline structure. Thus, the periodic nanostructures may have been formed by periodic etching and not by rearrangement.

With an average power of 2.0 W or greater, convex-folded microstructures with sizes larger than 2 μm were formed on the periodic nanostructures, as shown in the SEM images in Fig. 1. The formation of microstructures on titanium by femtosecond-laser irradiation at high laser fluence has been reported [28]. Tsukamoto *et al.* reported that the microstructures were formed by an intensity modulation, which arose from the interaction of the laser and its scattered wave. In our research on irradiation of SiC, we discuss the

crystalline state of the microstructures by TEM observation. The TEM images of the sidewall region of SiC irradiated at an average power of 4 W and a repetition frequency of 1000 kHz are shown in Fig. 4. As shown in the bright-field TEM image in Fig. 4(a) and the dark-field TEM image obtained with (0006) reflections in Fig. 4(b), the core of the periodic nanostructures below the microstructures remained crystalline, as was the case in Fig. 3. The microstructures that covered the periodic nanostructures were amorphous and extended from the amorphous SiC layer that covered the periodic nanostructures. The density of the microstructures was lower than that of the amorphous SiC layer that covered the periodic nanostructures. The present TEM results suggest that the amorphous region covering the periodic nanostructures grew through interaction with ambient gases during laser irradiation at high laser power. Then, some of the grown-amorphous regions coalesced with each other to form larger structures. Formation of these microstructures with high reproducibility has the potential to be widely applied. Controlling the crystalline state and the size are the current issues.

The depth of the v-shaped ablation trench as a function of the average laser power is shown in Fig. 5, at various peak intensities in Fig. 5(a) and at a constant peak intensity of 2.6 TW/cm^2 in Fig. 5(b). With increasing peak intensity, the depth of the v-shaped ablation trench increased. As shown in Fig. 5(b), the depth of the ablation trench also increased with increasing average power at constant peak intensity. The effect of average power is larger than that of repetition frequency, in view of the results shown in Fig. 5(a). Responding to previous reports in which the crystalline state of Si was affected by surface roughness [8] and the number of superimposed pulses [18, 19], detailed investigations of the laser-induced periodic structures on SiC will be conducted to clarify the formation mechanism of highly controlled nano- and micro-periodic structures in the future. This

will enhance the surface functionalization of semiconductor devices, especially in the area of optoelectronics.

4. Conclusion

In this study, we investigated the configuration and crystalline states of femtosecond-laser-induced periodic structures on SiC using SEM and TEM. The core of the periodic nanostructures retained a high crystalline quality similar to that of the SiC substrate. Under high-power laser irradiation, microstructures with sizes larger than 2 μm were formed on the periodic nanostructures. The microstructures were amorphous and it is thought that they grew through interaction with ambient gases during laser irradiation at high laser power.

Acknowledgements

The authors would like to acknowledge IMRA America Inc. for the opportunity to use the femtosecond laser oscillator. This work was supported by the Inter–university Cooperative Research Program of the Institute for Materials Research, Tohoku University (Proposal No.16K0056), JSPS KAKENHI Grant–in–Aid for Scientific Research on Innovative Areas Grant Number JP16H06415, JSPS KAKENHI Grant-in-Aid for Young Scientists (B) Grant Number JP17K14111, and JSPS KAKENHI for Scientific Research (B) Grant Number JP15H03535. High-resolution TEM was performed by Dr. Hideto Yoshida under the Research Program of "Dynamic Alliance for Open Innovation Bridging Human, Environment and Materials" (#20173054) in "Network Joint Research Center for Materials and Devices".

References

[1] S. Nakamura, K. Sugioka, and K. Midorikawa: Appl. Phys. A 101 (2010) 475.

[2] S. Maruo and J. T. Fourkas: Laser Photonics Rev. 2 (2008) 100.

[3] M. Hashida, A. F. Semerok, O. Govert, G. Petite, Y. Izawa, and J. F. Wagner: Appl. Surf. Sci. 197-198 (2002) 862.

[4] J. Bonse, J. Kruger, S. Hohm, and A. Rosenfield: J. Laser Appl. 24 (2012) 042006.

[5] L. Gemini, M. Hashida, M. Shimizu, Y. Miyasaka, S. Inoue, S. Tokita, J. Limpouch, T. Mocek, and S. Sakabe: J. Appl. Phys. 114 (2013) 194903.

[6] R. Miyagawa, Y. Okabe, Y. Miyachi, M. Miyoshi, T. Egawa and O. Eryu: Trans. Mater. Res. Soc. Jpn. 42(2) (2016) 155.

[7] G. Miyaji, K. Miyazaki, K. Zhang, T. Yoshifuji, and J. Fujita: Opt. Express 20 (2012) 14848.

[8] T. Tomita, R. Kumai, H. Nomura, S. Matsuo, S. Hashimoto, K. Morita, and T. Isu: Appl. Phys. A 105 (2011) 89.

[9] G. Miyaji and K. Miyazaki: Opt. Express 16 (2008) 16265.

[10] M. Yamaguchi, S. Ueno, R. Kumai, K. Kinoshita, T. Murai, T. Tomita, S. Matsuo, and S. Hashimoto: Appl. Phys. A 99 (2010) 23.

[11] N. Yasumaru, K. Miyazaki, and J. Kiuchi: Appl. Phys. A 76 (2003) 983.

[12] T. J. –Y. Derrien, T. E. Itina, R. Torres, T. Sarnet, and M. Sentis: J. Appl. Phys. 114 (2013) 083104.

[13] R. L. Harzic, D. Dörr, D. Sauer, F. Stracke, and H. Zimmermann: Appl. Phys. Lett. 98 (2011) 211905.

[14] T. Jia, H. Chen, M. Huang, F. Zhao, J. Qiu, R. Li, Z. Xu, X. He, J. Zhang, and H. Kuroda: Phys. Rev. B 72 (2005) 125429.

[15] A. Borowiec and H. K. Haugen: Appl. Phys. Lett. 82 (2003) 4462.

[16] S. Sakabe, M. Hashida, S.Tokita, S. Namba, and K. Okamuro: Phys. Rev. B 79 (2009) 033409.

[17] Y. Izawa, Y. Setuhara, M. Hashida, M. Fujita, and Y. Izawa: Jpn. J. Appl. Phys. 45 (2006) 5791.

[18] T. H. R. Crawford, J. Yamanaka, G. A. Botton, and H. K. Haugen: J. Appl. Phys. 103 (2008) 053104.

[19] T. H. R. Crawford, J. Yamanaka, E. M. Hsu, G. A. Botton, and H. K. Haugen: Appl. Phys. A 91 (2008) 473.

[20] M. Budiman, E. M. Hsu, H. K. Haugen, and G. A. Botton: Appl. Phys. A 98 (2010) 849

[21] Y. M. Tairov and V. F. Tsvetkov: J. Cryst. Growth 43 (1978) 209.

[22] J. Takahashi and N. Ohtani: Phys. Status Solidi B 202 (1997) 163.

[23] R. T. Leonald, Y. Khlebnikov, A. R. Powell, C. Basceri, M. F. Brady, I. Khlebnikov, J. R. Jenny, D. P. Malta, M. J. Paisley, V. F. Tsvetkov, R. Zilli, E. Deyneka, H. M. Hobgood, V. Balakrishna, and C. H. Carter, Jr.: Mater. Sci. Forum 600-603 (2009) 7.

[24] K. Hotta, K. Hirose, Y. Tanaka, K. Kawata, and O. Eryu: Mater. Sci. Forum 600-603 (2009) 823.

[25] R. Miyagawa and O. Eryu: Proc. 7th Int. Symp. Advanced Science and Technology of Si Material, 2016, p.276.

[26] T. Okada, H. Kawahara, Y. Ishida, R. Kumai, T. Tomita, S. Matsuo, S. Hashimoto, M. Kawamoto, Y. Makita, and M. Yamaguchi: Appl. Phys. A 92 (2008) 665.

[27] M. E. Levinshtein, S. L. Rumyantsev, and M. S. Shur: Properties of Advanced Semiconductor Materials: GaN, AlN, InN, BN, SiC, SiGe (Wiley, Ner York, 2001)

[28] M. Tsukamoto, K. Asuka, H. Nakato, M. Hashida, M. Katto, N. Abe, and M. Fujita: Vacuum 80 (2006) 1346.

Figure 1

Cross-sectional SEM images of the 6H-SiC substrate irradiated by scanning with a femtosecond laser. High-resolution image of (a) the nanostructures formed by 0.5 W and 500 kHz irradiation and (b) the microstructures on the nanostructures formed by 4.0 W and 1000 kHz irradiation.

Figure 2

Periodicity of laser-induced periodic nanostructures on 6H-SiC.

Figure 3

TEM images of the 6H-SiC substrate irradiated at 0.5 W and 500 kHz:

(a) bright-field TEM image, (b) high-resolution TEM image, and (c) diffraction pattern.

Figure 4

TEM images of 6H-SiC substrate irradiated at 4 W and 1000 kHz:
(a) bright-field TEM image and (b) dark-field TEM image.

Figure 5

Depth of the v-shaped ablation trench as a function of average laser power: (a) repetition frequency as a parameter and (b) at a constant peak intensity of 2.6 TW/cm^2.

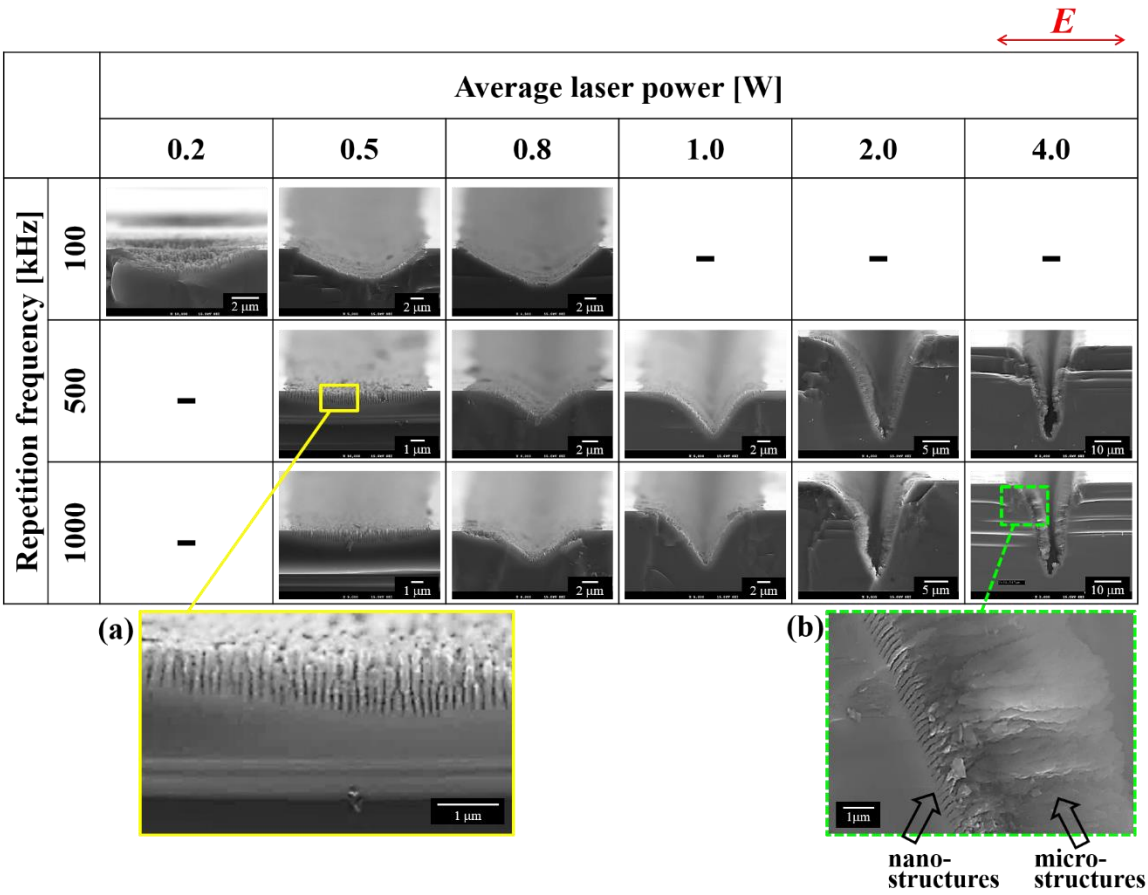

Figure 1 (Color online) Cross-sectional SEM images of the 6H-SiC substrate irradiated by scanning with a femtosecond laser. High-resolution image of (a) the nanostructures formed by 0.5 W and 500 kHz irradiation and (b) the microstructures on the nanostructures formed by 4.0 W and 1000 kHz irradiation.

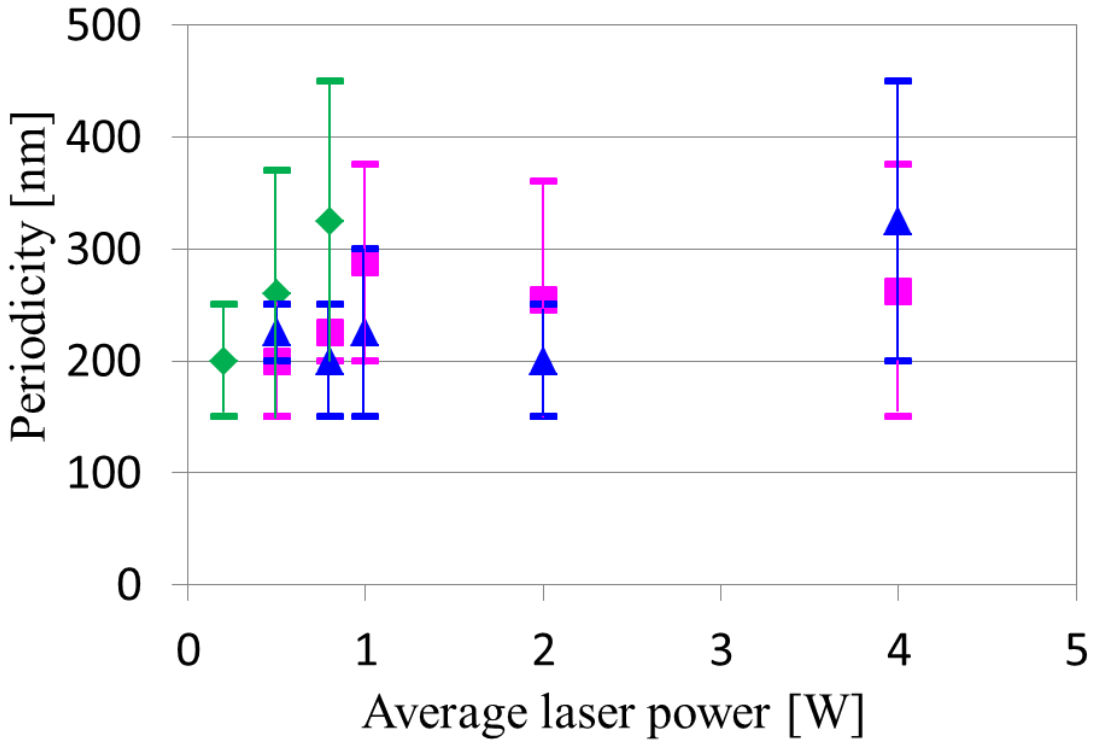

Figure 2 (Color online) Periodicity of laser-induced periodic nanostructures on 6H-SiC.

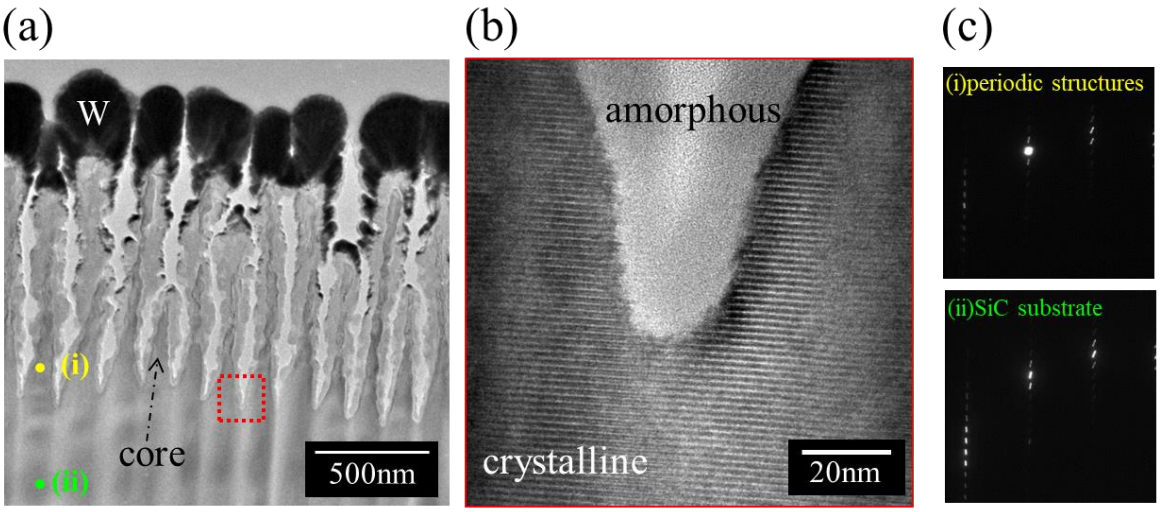

Figure 3 (Color online) TEM images of the 6H-SiC substrate irradiated at 0.5 W and 500 kHz:
(a) bright-field TEM image, (b) high-resolution TEM image, and (c) diffraction pattern.

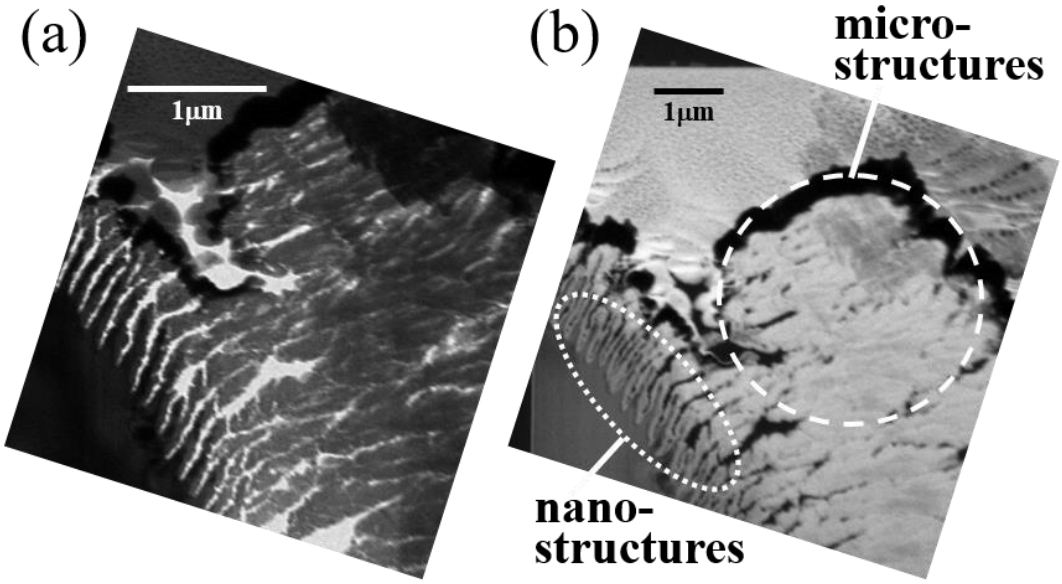

Figure 4 TEM images of 6H-SiC substrate irradiated at 4 W and 1000 kHz: (a) bright-field TEM image and (b) dark-field TEM image.

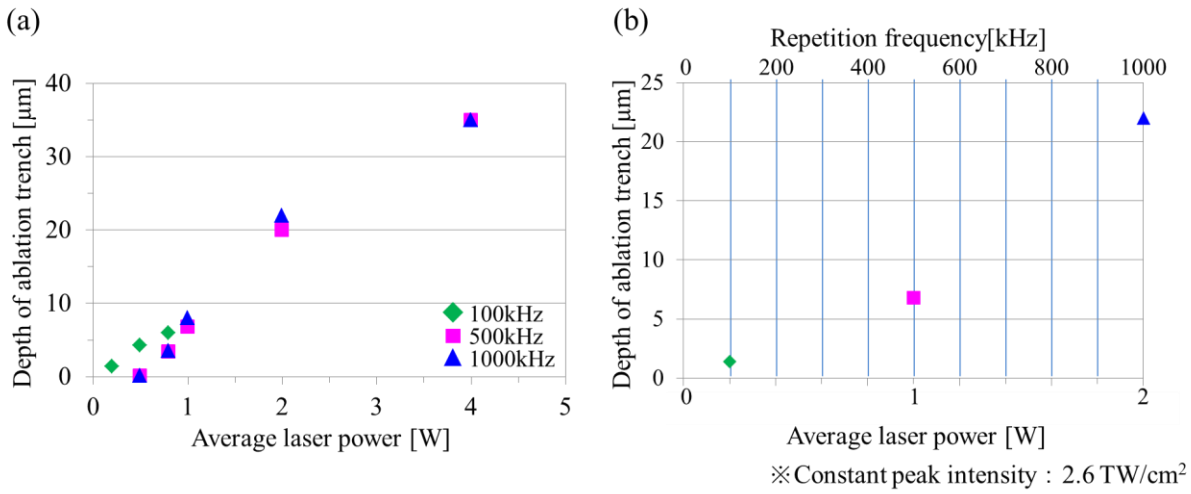

Figure 5 (Color online) Depth of the v-shaped ablation trench as a function of average laser power: (a) repetition frequency as a parameter and (b) at a constant peak intensity of 2.6 TW/cm^2.